

Cathodoluminescence color profile of radiation-damage halo in quartz by CCD image analysis

Yoshitada Horikawa* and Kosei Komuro

Introduction

Under cathodoluminescence (CL), light-colored halo is often seen in quartz adjacent to radioactive minerals. This halo is considered as radiation damage due to alpha particles because the width of halo matches with the calculated range of alpha particle (Owen, 1988). The CL color of the halo is generally stronger in red component (620–650 nm) compared to that of the host quartz, being considered to be attributed to recombination of electrons at non-bridging oxygen band (Siegel and Marrone, 1981; Götze *et al.*, 2001).

Descriptive studies for various occurrences revealed a wide variety of halos with different color structure. Owen (1988) observed quartz in contact to zircon in quartzite and found color zoning within halo, whose sizes are roughly explained by ranges of the parent and its daughter nuclides in ^{238}U series. In the study of sandstone-type uranium ores, halos are reddish to light bluish, some of which have distinct color zoning of reddish at the outside and bluish at the inside (Closel *et al.*, 1992; Komuro *et al.*, 1995). The color profile of halo is considered to be related to the profile of radiation damage which was simulated for various occurrences (Horikawa and Komuro, 1999), however, its description has not been reported up to now. Imaging by means of cooled CCD camera is able to register low-intensity CL conveniently with shorter time of exposure as compared to normal photographing. Its image analysis is expected to clarify the color profile of faint CL halo. Recently, the authors examined the relation between operating condition and appearance of CL halo in image taken by a cooled CCD camera and found most suitable operating condition for its recognition (Komuro and Horikawa, 2001). On the basis of the results, here we describe color profiles of some CL halos in quartz from sandstone-type uranium ores by CCD image analysis.

Samples

The samples used in this study are detrital quartz grains in sandstone-type uranium ores from the Kaneyamba deposit in Zimbabwe of Triassic to Jurassic in age. The ores consist of detrital grains mainly of quartz with feldspars

and matrices of hydromica minerals with uraninite, coffinite, pyrite and uraniferous organic matters (Komuro and Koyama, 1993; Komuro *et al.*, 1994).

Under CL, radiation-damage halo of about 30 μm is distinctly found in quartz, especially in high grade ores over 1 wt% U_3O_8 , but is also recognized in low grade sandstones of 0.02 to 0.1 wt% U_3O_8 (Komuro *et al.*, 1995). The width of halo generally agrees with the result of calculation by Owen (1988) but is somewhat larger due to the effect of sectioning as pointed out by Horikawa and Komuro (2000). On the basis of the mode of occurrence, halos can be grouped into three types: (i) halos of the marginal part of detrital quartz like rim, which are due to uraninite and coffinite in matrices, (ii) halos along the fractures in the detrital quartz, and (iii) ring halos in quartz in contact with specific mineral inclusion. The types (i) and (ii) are common, while the type (iii) is rare. In many cases, the existence of radionuclide-bearing minerals is difficult to discriminate in the types (ii) and (iii).

The halos are reddish to light bluish in color. The difference of color might be closely related to the concentration of radionuclides of adjacent radionuclide-bearing mineral, and the original color of the host quartz that might be due to the difference of the origin. The halos with high concentration tend to be reddish, whereas those with low concentration are light bluish. While brownish gray quartz grains tend to have reddish halos, grains of bluish gray show light bluish. Some halos have zonal color structure from bluish at the inside to reddish at the outside.

We describe here following three cases: (a) reddish halo of type (i) in a brownish gray quartz grain, (b) halo of type (i) with zonal color structure from bluish at the inside to reddish at the outside in a bluish gray quartz grain, and (c) reddish halo of type (iii) in a brownish gray quartz, from the high grade ores of 4.5 wt% U_3O_8 . The images under CL together with transmitted light taken by CCD camera are shown in Fig. 1.

Methods

The used CL unit was a Luminoscope® ELM-3R equipped with an Olympus BX-60 microscope furnished in a darkroom. The brightest beam condition without

* Doctoral Program in Geoscience, University of Tsukuba

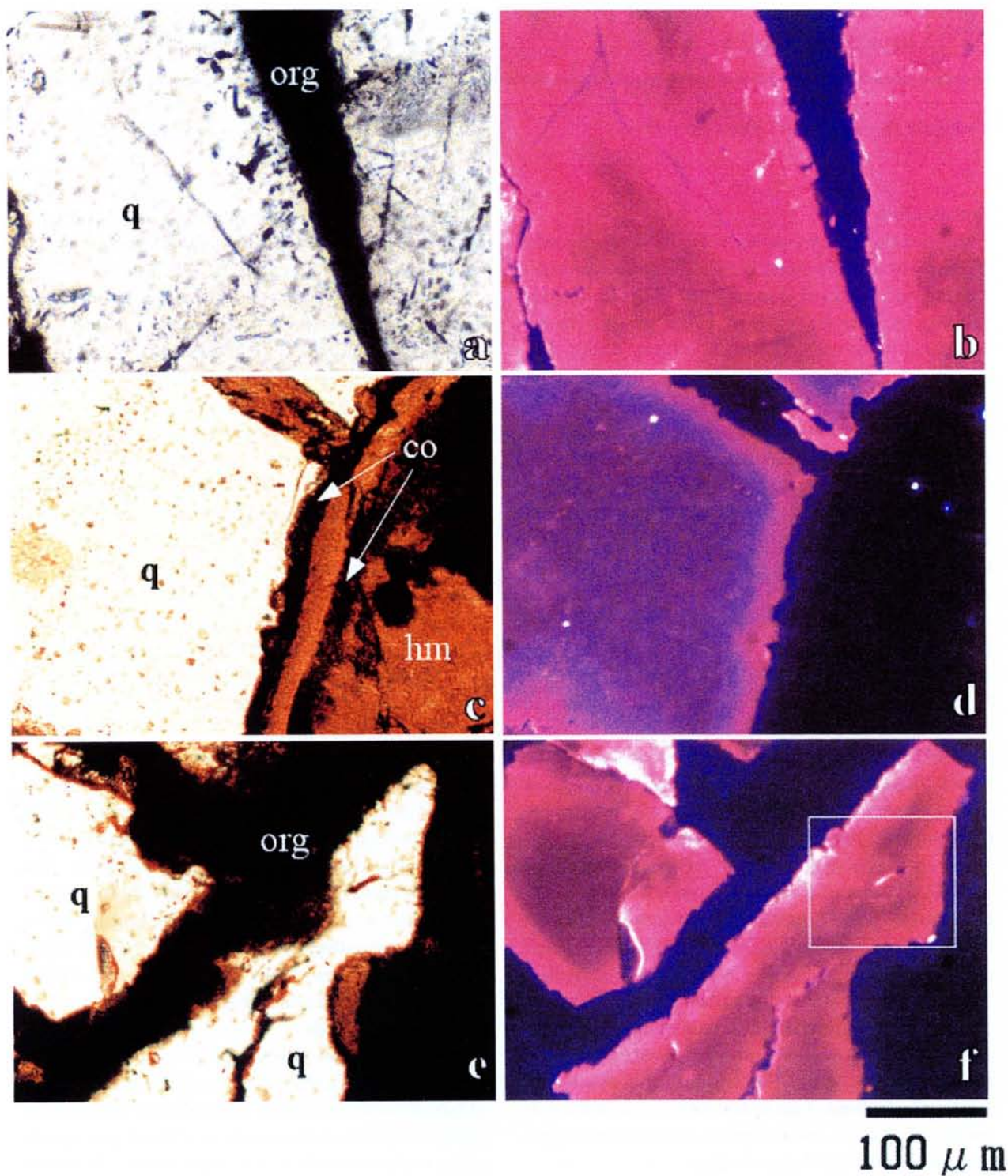


Fig. 1. CCD images of quartz grains with radiation-damage halos from the Kaneyamba ores of high uranium concentration of 4.5 wt% U_3O_8 . Transmitted (a) and CL (b) images of brownish-gray luminescing quartz with reddish halo. Transmitted (c) and CL (d) images of bluish-gray luminescing quartz with zonal halo with the colors of inner bluish and outer reddish. Transmitted (e) and CL (f) images of brownish gray quartz with ring halo around a radioactive mineral inclusion. The square in (f) indicates the portion of ring halo. Scale bar is 100 μ m. Abbreviations are, q: quartz, co: coffinite, hm: hydromica, and org: uraniferous organic matter.

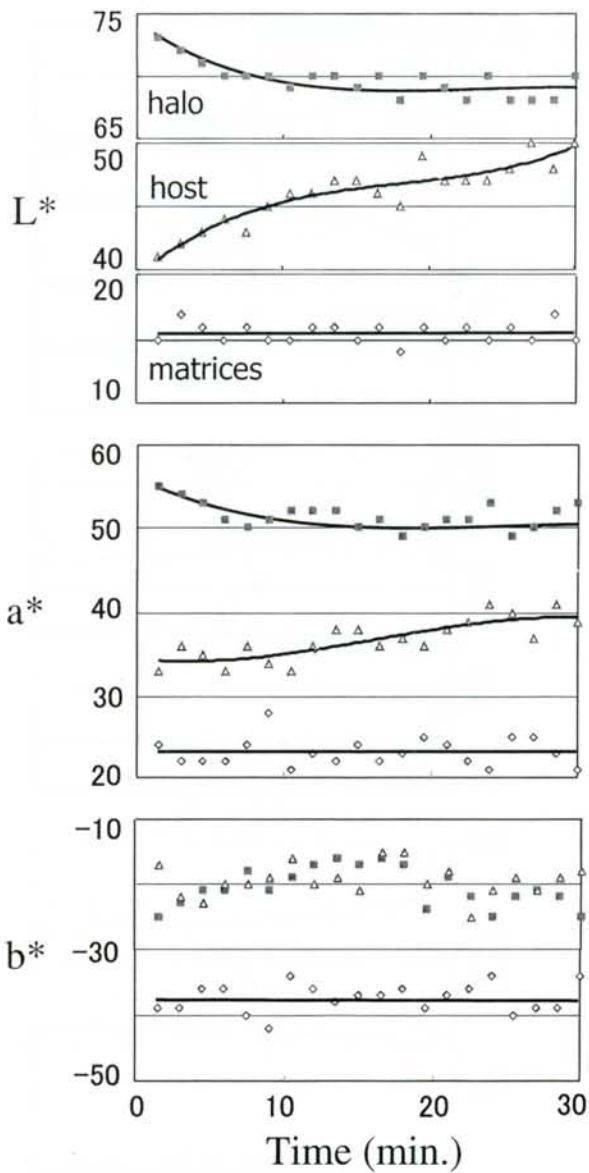


Fig. 2. Changes of L^* , a^* and b^* values with time for the reddish halo (■), the host brownish gray quartz (Δ) and the matrices (\diamond).

distinct beam damage shown in Komuro and Horikawa (2001) was adopted: beam voltage of 15 kV, beam current of 0.8 mA, and beam area of 27 mm². The generated CL was recorded as images taken by a Bitran BS-30C cooled CCD camera with the exposure time of 90 seconds. The obtained image data are firstly corrected by elimination of electric noises and background glimmer. The data originally denoted as the RGB space are corrected clearly visible at the same scale with keeping color balance and converted to the popular $L^*a^*b^*$ color space, in which the values of L^* , a^* and b^* represent lightness, redness (+)-greenness (-) and yellowness (+)-blueness (-), respectively. We use the L^* for the

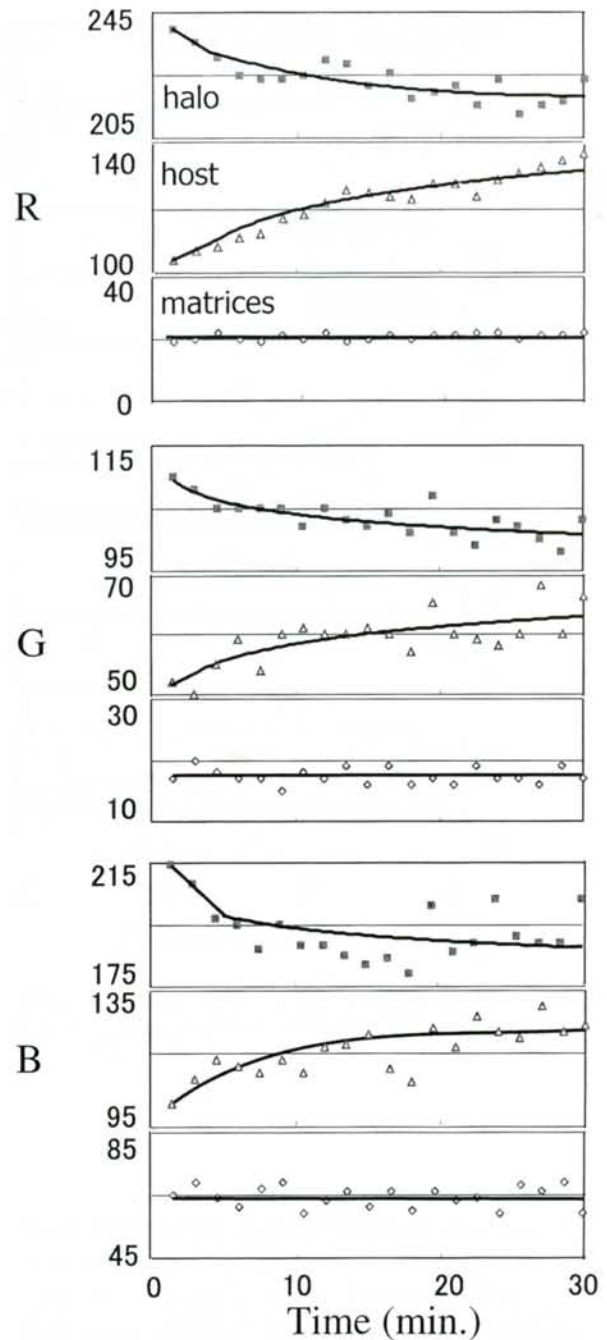


Fig. 3. Changes of R, G and B values with time for the reddish halo, the host brownish gray quartz and the matrices. Symbols are the same as in Fig. 2

brightness and the R, G and B for color in describing color profile. The image data analysis with repeating measurements suggests that the magnitude of experimental error is largest in b^* , next in a^* and third in L^* in the $L^*a^*b^*$ space, and largest in B, next in G and third in R in the RGB space. We present here raw data without smoothing.

The CL emission is known to change continuously

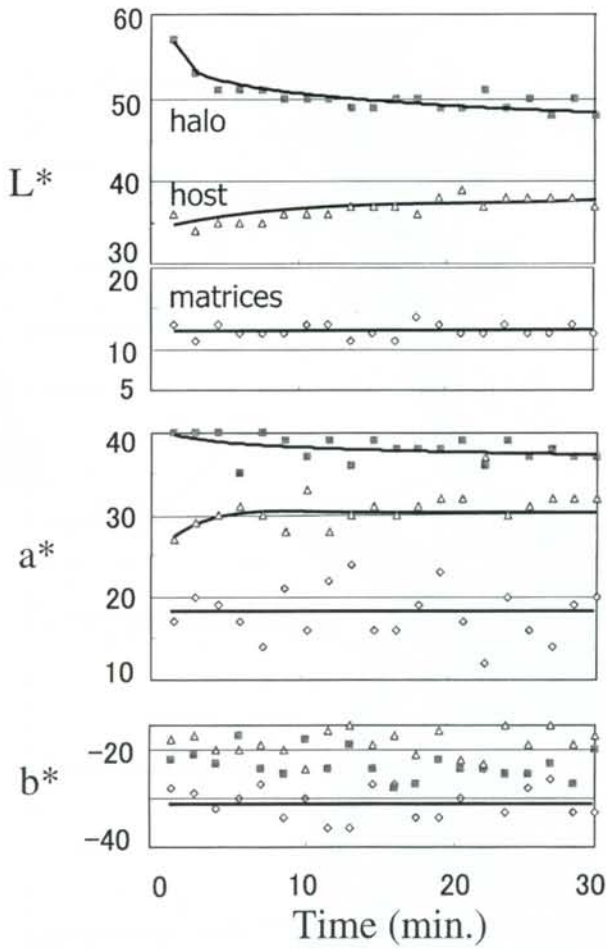


Fig. 4. Changes of L*, a* and b* values with time for the zonal halo (■), the host bluish gray quartz (△) and matrices (◇).

with time, in particular, in the start of the bombardment. Marshall (1988) mentioned that some quartz samples show an apparent CL which changes with time, especially of light bluish color that fades in intensity and changes color to red later. In this experiment, we recognized such changing phenomena, even in focusing or beam adjustment works. This indicates that CL color depends strongly on the irradiation time of the electron beam before imaging. In order to compare the halos of various occurrences, the measurement must be carried out under the same condition with irradiation time. We examined the changes of the color of halo, the host quartz and matrices of (a) and (b) with time by taking continuous images with the exposure time of 90 seconds, and decided the condition on irradiation time before imaging as 4 minutes (the reason is given below), under which was made description of color profile of halo.

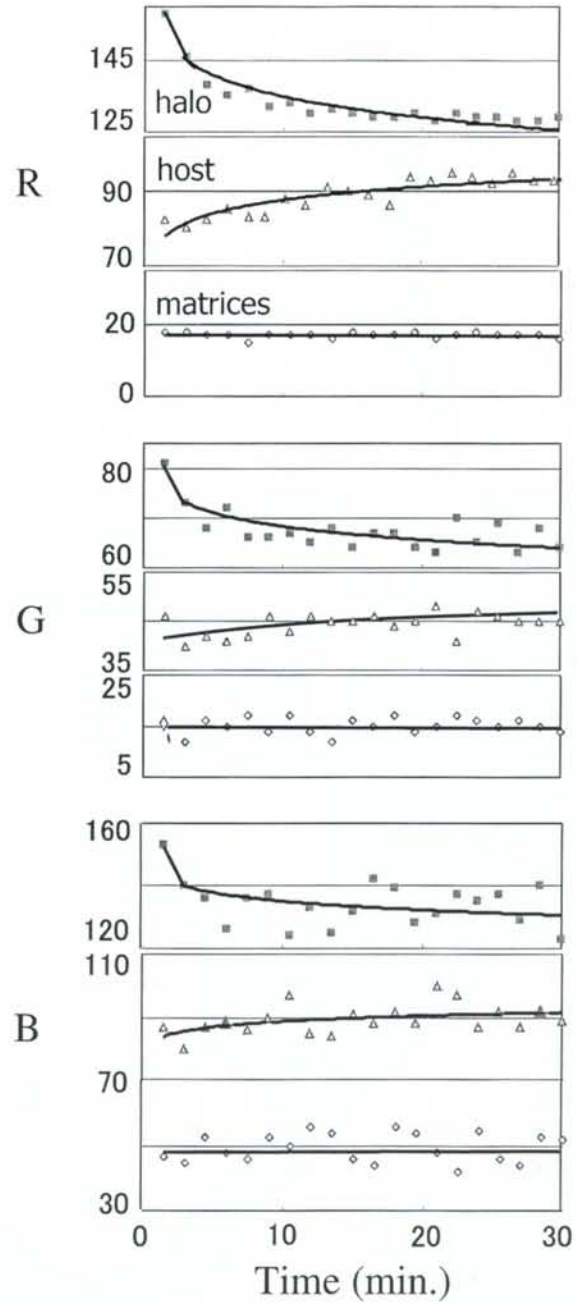


Fig. 5. Changes of R, G and B values with time for the zonal halo, the host bluish gray quartz and matrices. Symbols are the same as in Fig. 4.

Results and discussion

Change of color with time

The changes of L*, a* and b* values with time are shown in Figure 2 for the reddish-colored halo in the brownish gray quartz (a). Matrices mainly of uraniferous organic matter have the smallest L*, a* and b* values with the average of 15.6, 23.2 and -37.4, respectively. The values of L* and a* of the host quartz increase slightly with time, from 41 to 50, and 33 to 41, respectively, while

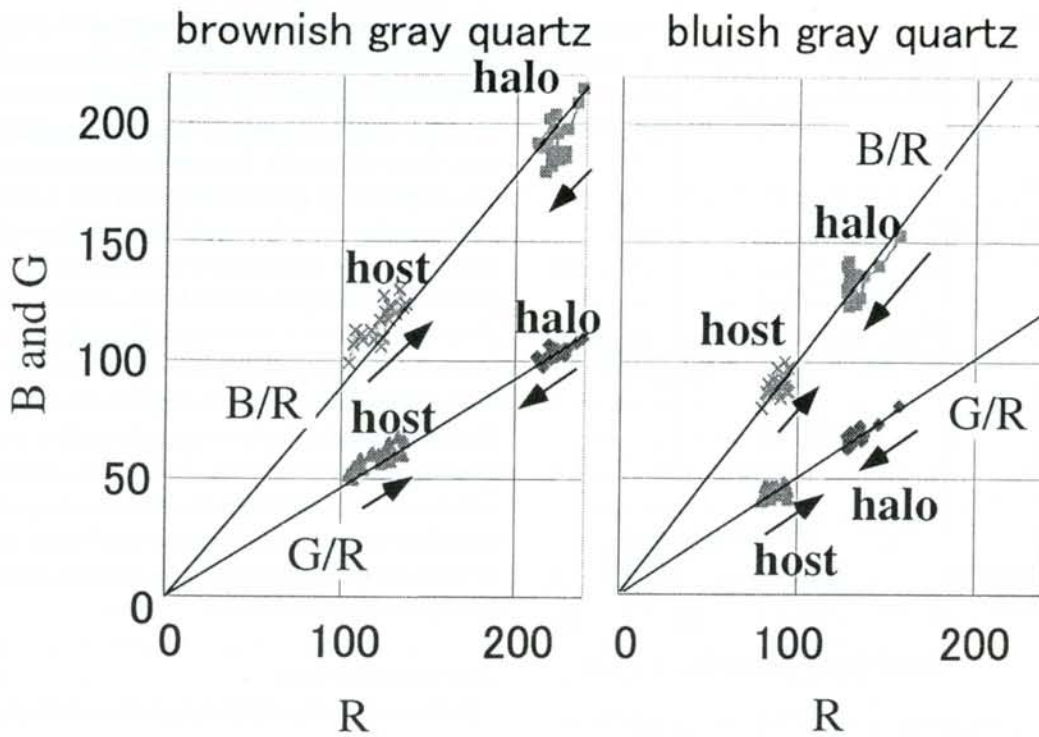


Fig. 6. The B/R and G/R ratios for the halos in brownish gray quartz and bluish gray quartz. Symbols are, \blacksquare : the B/R ratios for the halos, \times : the B/R ratios for the host quartz grains, \blacklozenge : the G/R ratios of the halos and \blacktriangle : the G/R ratios of the host quartz grains. The arrows indicate the direction of color change with time.

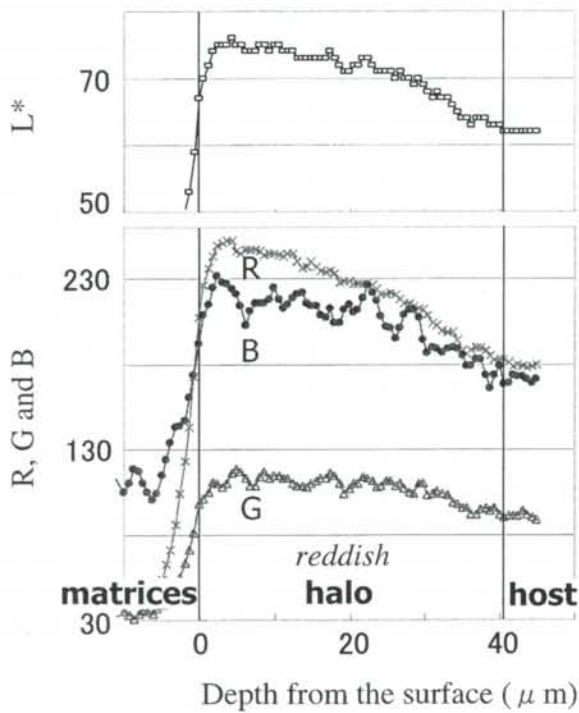


Fig. 7. CL color profile in the section of reddish halo in brownish gray quartz. The "0" of the horizontal axis means the position of the surface of quartz. Symbols are, \square : L^* , \times : R, \bullet : B and \triangle : G.

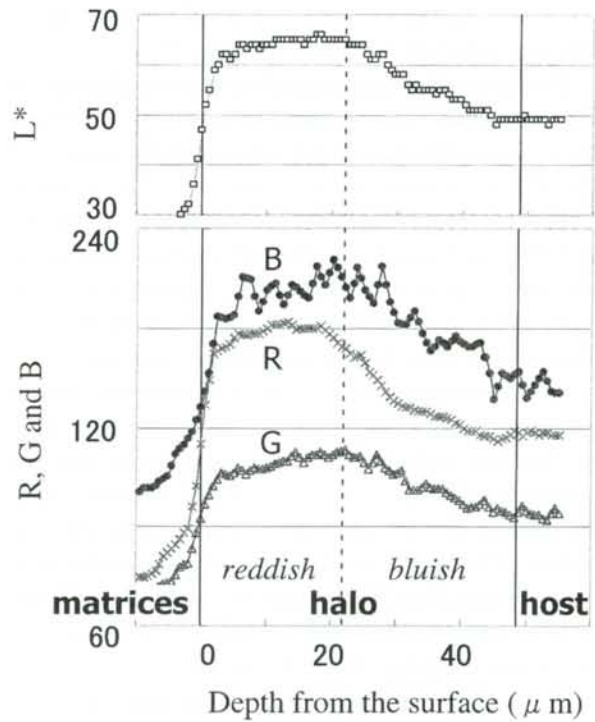


Fig. 8. CL color profile in the section of zonal structured halo in brownish gray quartz. Symbols are the same as in Fig. 7.

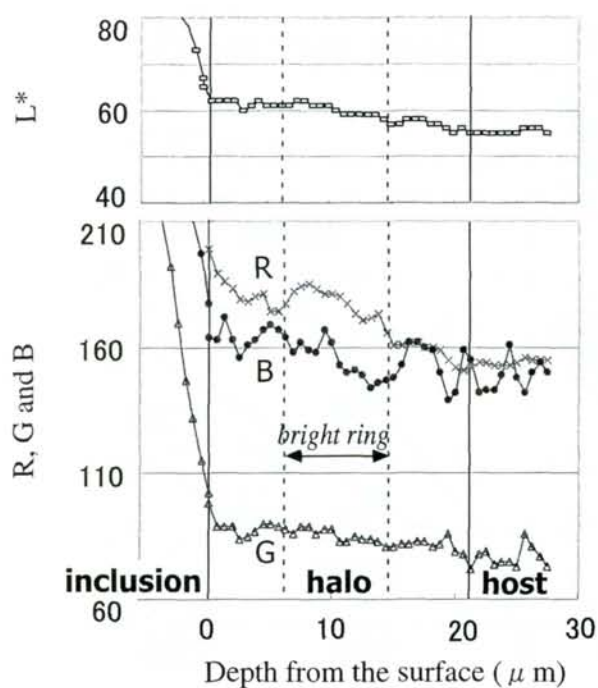


Fig. 9. CL color profile in the section of ring halo in the brownish gray quartz. Symbols are the same as in Fig. 7.

the b^* varies widely around -19.4 . The L^* and a^* values of halo decrease slightly with time, from 73 to 68, and 55 to 50, respectively, in particular the L^* in the first 5 minutes, while the b^* varies around -20.6 .

The R, G and B values based on the same data for (a) show clear color changes with time (Fig. 3). Matrices have the smallest R, G and B values with the average of 21, 17 and 64, respectively. The values of R, G and B of the host quartz increase slightly with time, from 104 to 137, from 50 to 66, and from 99 to 124, respectively. The R, G and B of halo decrease slightly with time, from 239 to 215, from 110 to 98, and from 214 to 189, respectively, in particular in the first 5 minutes.

The color change for the halo with zonal structure in bluish gray quartz (b) shows a similar tendency (Fig. 4). Matrices of hydromica minerals with coffinite and uraninite have the smallest L^* , a^* and b^* values with the average of 12.3, 18.1 and -31.6 , respectively. The values of L^* and a^* of the host increase slightly, from 34 to 38 and 27 to 32, respectively, while the b^* varies widely around -18.6 . The L^* and a^* values of halo decrease slightly, from 57 to 48 and 40 to 37, respectively, in particular the L^* in the first 3 minutes, while the b^* varies around -23.1 .

Figure 5 shows the color change of (b) as denoted by RGB space. Matrices have the smallest R, G and B values with the average of 17, 15 and 50, respectively.

The values of R, G and B of host increase slightly with time, from 80 to 93, from 40 to 45, and from 80 to 92, respectively, except for the higher values in the first 1.5 minutes. The R, G and B of halo decrease slightly with time, from 158 to 128, from 81 to 64, and from 153 to 123, respectively, particularly in the first 3 minutes.

The results strongly suggest that the CL emission of halo is stronger in the first 3-5 minutes and decreases gradually with time whereas that of the host quartz gradually increases with time. The color of the host deepens with time, but the color of halo fades without distinct change of the ratios of B/R and G/R (Fig. 6). The difference of color between halo and the host quartz becomes smaller with time. Taking the color stability with time and working time for focusing also into consideration, the condition on irradiation time of 4 minutes before imaging shown above is adopted for description of color profiles.

Color Profile of halo

In the section of reddish halo in brownish gray quartz (a), the L^* , R, G and B values decrease from the surface to inside, from 75 to 63, from 252 to 195, from 120 to 98, and from 232 to 190, respectively (Fig. 7). The gradients of the L and R are gentle near the surface, but gradually change steeper as it goes to inside. The profiles of the B and G are in saw-wave pattern but gradually decrease. The R prevails over the B and G throughout the profile, being consistent with the color image in Fig. 1b. The difference between the R and B is larger near the surface, but gradually decreases as it goes to inside.

The halo of zonal color structure in bluish gray quartz (b) has the L, R, G and B values that slightly increase from surface to 18 μm and decrease from 18 to 43 μm (Fig. 8). The L and R decrease markedly from 18 to 30 μm but gently from 30 to 43 μm . The B prevails over the R throughout the profile, but the difference is smaller from surface to 20 μm , which corresponds to reddish color part from the surface to 20 μm in image in Fig. 1d.

In the section of ring halo in the brownish gray quartz (c), the L^* , R, G and B values gently decrease from outside to inside with some peaks (Fig. 9).

The R of bright ring under CL image between 6 to 16 μm (Fig. 1f) is slightly higher. This agrees with the simulation that shows the damage intensity suddenly decreases around 16.6 μm , being due to the ranges of ^{238}U , ^{230}Th and ^{234}U (Horikawa and Komuro, 1999).

The relationship between color change and radiation

The foregoing color profiles show that the brightness of CL in halo decreases with distance. Recently,

Horikawa and Komuro (1999) simulated radiation-damages in quartz and found that the intensity of the radiation-damage generally decreases with distance although the occurrences of associated radionuclides bearing minerals strongly affect. Taking the results into consideration, the data indicates that the brightness of CL in halo increases with increasing of radiation. This suggests that the CL brightness in halos is expected to be a good dosimeter or a new dating tool that records radiation by alpha particles.

The CL color of halo is also strongly related with distance in the profiles. In the inside of the halo where radiation is lower, both the R and the B increase with increasing of radiation. In the outside where radiation is higher, on the other hand, the R obviously increases with the increase of radiation, relative to the B, leading to the reddish halo with higher concentration of radionuclides. These color values which might be correlated with different type of defects, are also expected to be a good dosimeter or a new dating tool. The image analysis of quartz after radiation experiment or that of natural samples combined systematically with dating and radionuclides microanalysis will provide key data responsible for making a dosimeter.

Acknowledgements

We are thankful to Prof. Y. Kajiwara of the Univ. of Tsukuba and Dr. S. Toyoda of Okayama University of Science for their continuous encouragement. This study was partly supported by the resources of REIMEI Research of JAERI (Japan Atomic Energy Research Institute) and by the JNC (Japan Nuclear Cycle Development institute) Cooperative Research Scheme on the Nuclear Fuel Cycle.

References

- Clozel, B., Komuro, K., Nakashima, S., Nagano, T., Masaki, N. and Hayashi, H. (1992): *Report of the Research Institute of Natural Resources, Mining College, Akita University*, **57**, 25-55.
- Götze, J., Plötze, M. and Habermann, D. (2001): *Mineralogy and Petrology*, **71**, 225-250.
- Horikawa, Y. and Komuro, K. (1999): *Ann. Rep., Inst. Geosci., Univ. Tsukuba*, **25**, 51-56.
- Horikawa, Y. and Komuro, K. (2000): *Ann. Rep., Inst. Geosci., Univ. Tsukuba*, **26**, 55-57.
- Komuro, K. and Koyama, K. (1993): *Ann. Rep., Inst. Geosci., Univ. Tsukuba*, **19**, 73-78.
- Komuro, K., Suzuki, S., Yamamoto, M., Ohtsuka, Y. and Koyama, K. (1994) *Ann. Rep., Inst. Geosci., Univ. Tsukuba*, **20**, 67-72.
- Komuro, K., Yamamoto, M., Fujiki, S., Fukushima, T. and Koyama, K. (1995): *Ann. Rep., Inst. Geosci., Univ. Tsukuba*, **21**, 65-69.
- Komuro, K. and Horikawa, Y. (2001): *Ann. Rep., Inst. Geosci., Univ. Tsukuba*, **27**, 25-31.
- Marshall, D.J. (1988): *Cathodoluminescence of Geological Materials*. Unwin Hyman, Boston.
- Siegel, G. H. and Marrone, M. J. (1981): *J. Non-Cryst. Solids*, **45**, 235-247
- Owen, M. R. (1988): *Geology*, **16**, 529-532.
- Smith, J. V. and Stenstrom, R. C. (1965): *J. Geol.*, **73**, 627-635.

Keywords: radiation-damage halo, radiation damage, CCD image, image analysis, cathodoluminescence, quartz, color profile.